INVESTIGATION OF ALTERATIONS CONTROLLED BY FRACTURES USING REMOTE SENSING TECHNIQUES, FRACTAL CHARACTERISTICS AND STATISTIC PARAMETERS IN THE BAJESTAN, EAST OF IRAN

Reyhaneh Ahmadirouhani[1], Behnam Rahimi[1*], Mohammad-Hassan Karimpour[2], Amin Beiranvand pour[3,4], Azadeh Malekzadeh-Shafaroudi2

[1]Department of Geology, Faculty of Science, Ferdowsi University of Mashhad, Iran

[2]Research Center for Ore Deposit of Eastern Iran, Ferdowsi University of Mashhad, Iran

[3]Geoscience & Digital Earth Centre (INSTeG), Universiti Teknologi Malaysia, 81310 UTM Johor Bahru, Malaysia

[4]Korea Polar Research Institute (KOPRI), Songdomirae-ro,Yeonsu-gu, Incheon 21990,Republic of Korea

Email: beiranvand.amin80@gmail.com,ahmadirouhani.reyhaneh@mail.um.ac.ir

KEY WORDS: Alteration**,** Fractal, Fractures map, Remote sensing, Bajestan, Iran

ABSTRACT

The Bajestan is located in the north of the Lut block, the biggest structural block in the eastern Iran. ASTER data processing through Spectral Angle Mapper classification, band ratio, and band composition methods enhanced main the alteration zones, including Propylithic, Sericitic, Argillic and Fe-oxide alterations. Fractures map was prepared using SPOT-5 imagery and applying the enhanced spatial filters in order to recognize the role of fractures in controlling mineralization. Based on fracture map obtained by remote sensing and field studies, fractal pattern was examined through box-counting algorithm. The results showed that the maximum amount of the fractal dimension is observed in NW-SE orientation. Statistical parameters of fractures such as density, intensity, and fractures' intersection confirmed the results of previous fractal studies. Total data indicate that most alteration zones are related to lineaments, especially the main NW-SE faults. In addition, this study signifies the maximum probability of the occurrence of mineralization.

1. INTRODUCTION

Remote sensing has been used in a variety of geological studies e.g. mapping minerals (Sabins 1999; Vincent 1997; Di Tommaso and Rubinstein 2006; Abdi and Karimpour 2012; Karimpour et al. 2008; Eshghi Molan et al. 2014). Remote sensing techniques could be applied to recognize intact as well as altered rocks because their reflectance spectra are different from each other (Sabins 1999). One of the key ideas of remote sensing techniques in mineral exploration geology is that it is applied to rocks, minerals, and structures associated with a particular ore, and not the ore itself. These reasons are all way relevant (Vincent 1997).

The investigated area is situated within the northern part of the Lut Block, the main and biggest block in the east of Iranian micro-continent plate. The micro-continent of Central Iran has located in Alps-Himalaya belt, between the two northern and southern orogeny belts as well as the two Palaeothetys and Neothetys suture zones in the north and south, respectively. Active tectonics in the micro-continent of Central Iran is believed to be a result of convergence between the Arabian and Eurasia Plates.(Jackson et al. 1995).

Eastern Iran and particularly the Lut Block, has great potential for different types of mineralization as a result of its past subduction events, which led to extensive magmatic activity forming igneous rocks with different geochemical compositions. The Lut Block is characterized by extensive exposure of Tertiary volcanic and subvolcanic rocks formed due to the subduction prior to the collision of the Arabian and Asian plates (Camp and Griffis 1982; Tirrul et al. 1983; Berberian et al. 1999). The Lut Block extends over 900 km in a north-south direction and is only 200 km wide in an east-west direction. It is confined by the Nayband Fault and Shotori Range in the west. Different types of

metal ore bodies, such as porphyry Cu, Cu–Au–Fe-oxide, vein type, massive sulfide, Au-epithermal, intrusion-related gold systems and Sn–W-skarns and also non-metal have already been documented in the Lut Block (Karimpour et al. 2008).

Most of the study area is covered by upper cretaceous granitoid rocks including monzogranite, alkali granite, granodiorite and diorite. Metamorphic rocks including slate and phyllite are present in the north of the area. Skarns are observed in contact with fault zones and intrusive bodies in north and east of the area. Marble and hornfels, also exist adjacent to the intrusive bodies. Eocene volcanic rocks with andesite and andesibasalt composition are located in the east and north east of the area (Fig. 1).

Studied area as a part of the Lut Block, has many potentials for mineralization. Cu, Fe, Au and Barite mineralization along the alteration zones can be observed. The most important anomaly is Kalat-e-Kook with Cu mineralization in the southeast of the area. Mineralization in this rock has chiefly occurred in fractures and breccia zones mainly in the form of pyrite and chalcopyrite. Mineralization from this area has continued arriving in Kalat-e-Obi in the west of Kalat-e-Kook as skarnization (Fig. 1).

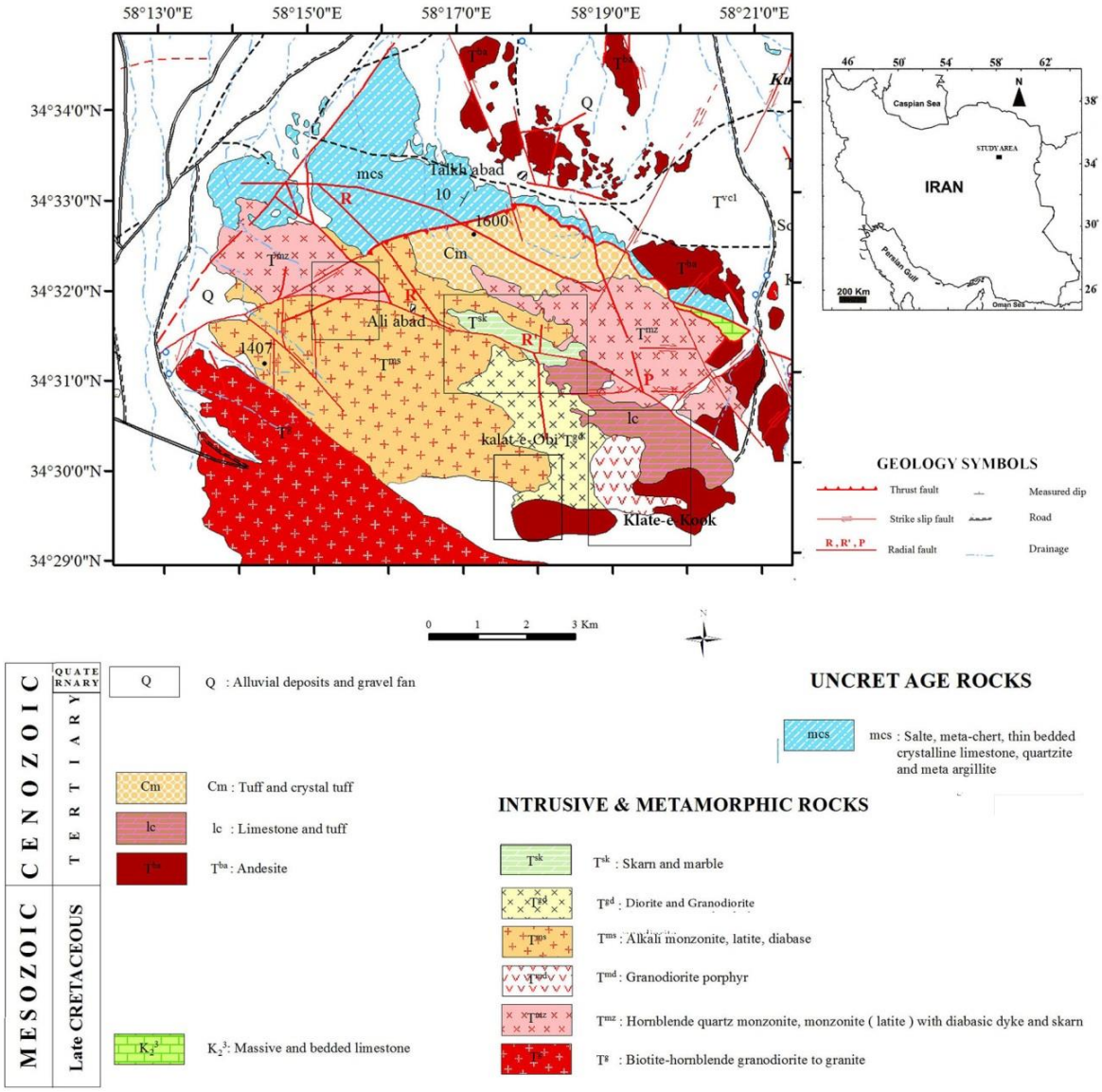

Figure 1. Simplified regional geological map of study area (modified and compiled from two 1:100.000 scale maps: Bajestan map (Ashoori et al. 2008) and Ferdows map(Pourlatifi 2002). Locations of anomalies are shown with rectangles.

In this research, ASTER and SPOT data were used as the base data to: enhance alteration zones, enhance fractures and prepare fractures map using enhancement spatial filters, applying fractal pattern on the resulted fractures map to determine fractal dimension and prepare fractal map and also statistics maps (density, intensity and fracture intersection).

The latter is applied to: identify effective alteration zones and their variety associated with mineralization, understand the mechanism of faults performance and structural evolution in the study area. The results of the alteration and fractures' mapping were checked out in-situ to verify the result of image processing.

2. MATERIALS AND METHODS

2.1 Remote sensing data

In this study, ASTER images were applied in order to enhance and separate the alteration zones and their varieties and recognize their relation to mineralization.

ASTER has some significant characteristic in geological mapping applications(Di Tommaso and Rubinstein 2006; Ninomiya 2002; Ninomiya 2004; Rowan et al. 2003; Rowan and Mars 2003; Pour and Hashim 2012). It is the first multispectral space borne sensor that can identify and discriminate hydrothermal alteration minerals in SWIR region (shortwave infrared) of the electromagnetic spectrum (Abrams and Hook 2000), ASTER VNIR (visible and near infrared) can provide sufficient capability for identification of vegetation and iron oxide minerals on surface and ASTER TIR (thermal infrared) data can map carbonates and silicates (Bedell 2001; Ninomiya 2003; Rockwell and Hofstra, 2008). Some scholars have applied many methods on ASTER data as a tool for mapping hydrothermal alteration mineral zones associated with copper and gold mineralization and the lithology of the related host rock (Di Tommaso and Rubinstein 2006; Rowan and Mars 2003; Yamaguchi and Naito 2003; Velosky et al. 2003; Hewson et al. 2005; Mars and Rowan 2006; Tangestani et al. 2008; Pour et al. 2011).

The data used in this study was ASTER level 1B data acquired on 29 June, 2000; In order to remove the optical leak from band 4 to the other SWIR bands, crosstalk correction algorithm was applied to SWIR bands (Iwasaki and Tonooka 2005).

In addition, SPOT-5 data with superior features compared to Landsat data were applied to enhance lineament and prepare the fractures map. Obtaining the base of fractures map from the SPOT data, fractal analysis and statistics parameters were calculated. SPOT-5 Image with ID: SPOTCOV_IRC_N34E058-A and 2007-10-16 dataset production date and spatial resolution of 2.5-metre was used in this research. The data geometrically and radiometrically were corrected. 2.5-metre colour image are obtained by merging two separate images, one in panchromatic mode at 2.5-metre resolution and the other in three-band multispectral mode at 10-metre resolution. Because the 2.5-metre image is, itself generated by merging two 5-metre images, one of the HRG instruments has to acquire three images simultaneously to produce a 2.5-metre colour image. Images, thus, obtained are like a three-band colour image, with a resolution of 2.5-meters and panchromatic viewing geometry (www.spotimage.com).

2.2 Data analysis

In order to determine the alteration zones in the study area, some image processing techniques as band composition, band ratio and SAM classification were performed on ASTER data.

The VNIR-SWIR regions of L1B dataset of the area were radiometrically normalized using the Log Residual (LOG) to remove the effects of sensor errors and environmental factors (Abdi and Karimpour 2012). A subset corresponding to the study area with 1152 x 821 pixels was derived for analytical procedures. From the nine band data set of ASTER data, a lot of approaches have been undertaken for the differentiation and mapping the surface mineral suites. In order to identify alteration zones in the area, SWIR colour composition in RGB: 468 was used (Di Tommaso and Rubinstein 2006) (Fig. 2a). This composition shows the Bajestan alteration zones in different colours. chlorite and epidote minerals related to propylithic alteration, are dark to bright green, clay minerals and sericite are showed in magenta and carbonate unites including skarns are yellow.

Enhancing alteration zones in this area by SAM method was implemented for Fe-alteration minerals (limonite, hematite, jarosite and goethite) and hydrothermal alteration minerals (muscovite as serecite, montmorillonite, alunite, kaolinite, illite, chlorite and epidote). Due to the overlap of representing similar minerals spectral in every alteration zone, only one mineral is represented (fig 2b).Selecting these minerals was carried out on the basis of anomaly types and alteration zones which observed in field studies.

The ASTER mineral mapping for Fe-alteration helped identify high intensity for hematite in the west of the prospect area (Fig. 2b). Moreover, for hydrothermal minerals, results showed high intensity for propylithic alteration minerals (chlorite and epidote) and clay minerals (kaolinite) in the east and north of the area (Fig. 2b).

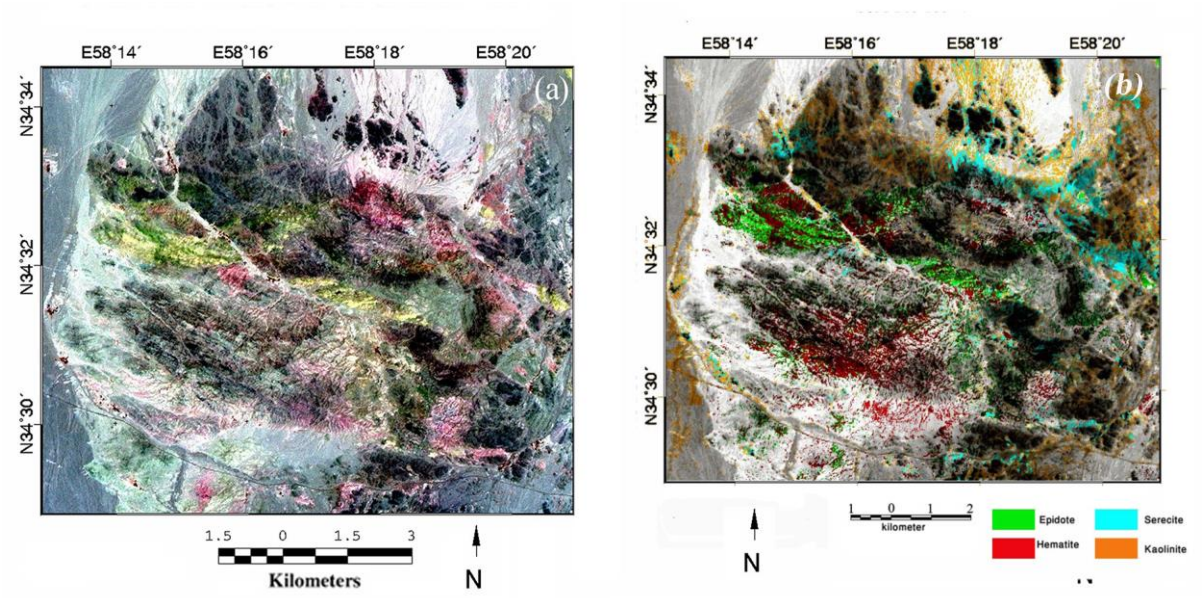

Figure. 2 (a) ASTER band combination in RGB: 468. The propylithic zones outlined in green, sericite and clay minerals are shown in magenta and carbonate units are characterized by yellow and (b) Spectral Angel Mapper(SAM) classification for selected minerals(epidote, hematite, kaolinite and serecite= muscovite), for presenting alteration zones: Fe oxide(hematit), propylithic (epidote), Phyllic(muscovite) and argillic(kaolinite).

SPOT-5 data processing used to prepare the Fractures Map to help recognize the probability of relation between fractures and alteration. For this aim, after making a RGB colour image, spatial filters e.g. High Pass, directional and standard filters were applied (fig.3a). Also directional filter were applied by 45 degrees angle (N 45 orientation) and other complementary processes for further enhancement. Finally, the main fractureswere plotted digitally (as a shapefile) by ArcMap software on SPOT-5 image as fracture map (fig 3b).

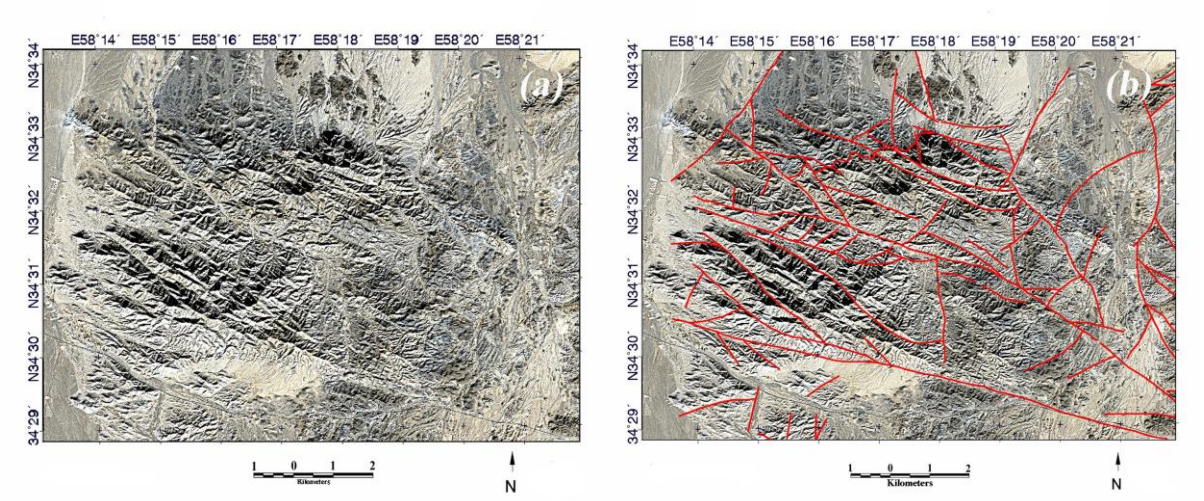

Figure. 3. (a) Resultant image map derived from the high pass filters and directional filter (b)Lineaments features in the Bajestan area that enhanced digitally by filtering methods.

Fractal analysis was done in area in order to better understand the quantitative analysis of the spatial and scaling characteristics of fractures, fractures' permeability, fractures' connections and their role in forming the hydrothermal alteration zones.

For Fractal analysis, the presence or absence of a fractal model for fractures network in the study area was examined through the “box counting” method. The “box counting” method was used based on the fractures map obtained from the remote sensing techniques and field studies. “Box counting” is the most common method used by many researchers (Cello, 1997; Fagereng, 2011; Hirata, 1989; Liu et al., 2015; Mandelbrot, 1983; Ram & Roy, 2005; Turcotte, 1992).

The results of these studies show fractures have fractal geometry in this area. The fractal dimension varies between 1.08 and 1.57 with an average of 1.35.To comparing the results of fractal dimension amounts by means of hydrothermal alteration zones and other data, the contour map derived from the distribution of fractal dimension was drawn (see Fig. 4a).

On the basis of the fractures map derived from SPOT-5 imagery analysis and field data, two fracture trace parameters were measured for the study area, including the fracture trace intensity and the fracture trace density. The trace intensity is defined as the total length of traces per unit area; the trace density is defined as the number of trace centers per unit area. The results of this step are two contour maps which evaluate the fracture trace intensity (see Fig. 4b) and fracture trace density (see Fig. 4c).

The calculation of fractures intersection also can help to identify the possibility and the prospective capability of creating fluid pathways. It has been widely recognized that faults have the enormous capability of creating efficient fluid pathways in the crust, which is otherwise relatively impermeable (Knipe, 1993; Sibson, 1994). To achieve these factors in the study area, after finding the intersections of fractures on the fracture map, the final plot as contour map was drawn (Fig. 4d).

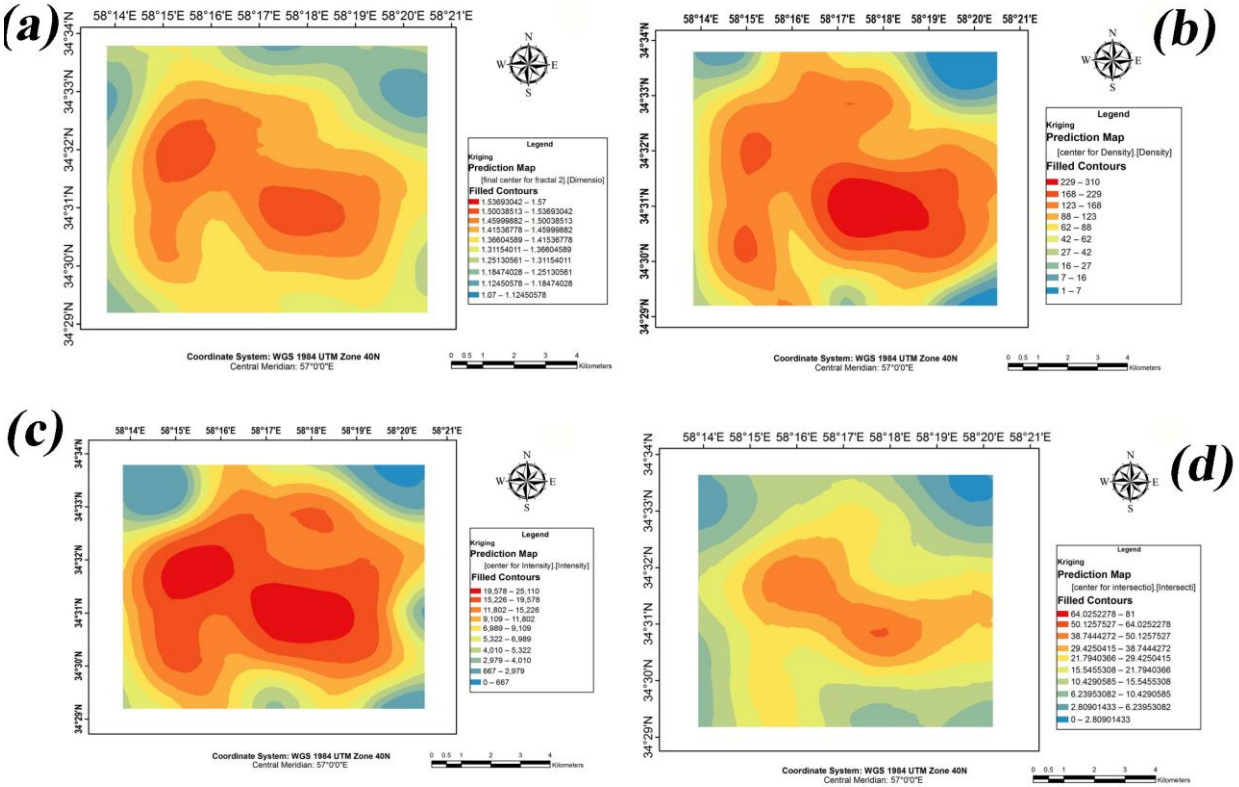

Figure.4 Contour map: (a) derived from the distribution of fractal dimension in the Bajestan, (b fractures intensity, (c) fractures density and (d)fracture intersection

3. RESULTS AND DISCUSSION

In this research, SPOT and ASTER satellite data processing, was carried out in several steps to identify areas with high probability of mineralization. For this purpose, alteration zones and its variants were identified in the region using remote sensing techniques such as: band composition and spectral angel mapper on ASTER multi band data. ASTER processing approach shows the extent of propylithic alteration particularly between the granitoid bodies and metamorphic (slate and phyllite) units which are lying east-west and northwest-southeast directions. Besides, this alteration along with phyllic and argillic alterations are clearly visible in Kalat-e-Kook and south of Kalat-e-Obi areas (Fig. 1). According to the evidences of copper mineralization observed in the field studies in these two regions and considering existence of the phyllic and argilic alteration zones in the center, all have been surrounded by propylithic alteration in Kalat-e-Kook prospect, presence of a hydrothermal alteration system which associated with Porphyry copper deposits in this region makes sense and it seems that skarn mineralization was formed (as exoskarn) in the south of Kalat-e-Obi is related to this system.

Fractures map was prepared using SPOT-5 imagery to determine the role of fractures in transportation of fluid flow and control of hydrothermal mineralization. Satellite data and field data determined two main regular fractures with simple shear structural style in Strike slip systems in the area. Two main orientations (NW-SE and NWW-SEE) are compatible with many of alteration zones.

In order to recognize and analyze fractures and their characteristics like fractures' permeability & connectivity and the role of them in forming alteration zones, base of fracture map was obtained from SPOT-5 data processing, fractal analysis in the study area was also implemented.

Hirata (1989) suggests that the upper limit of the fractal dimension of rock fracture geometry is about 1.6. The results of these studies show fractures have fractal geometry in this area and the fractal dimension varies between 1.08 and 1.57 with an average of 1.35. Fractal dimension amounts increase in two locale: northwest and southeast of the area. The concentration of high levels of fractal dimension in the of study area represents more evolution with structural deformation and development of fault branches along these directions. High fractal dimension shows increase in the fracture permeability, fractures connectivity and more brittle lithology (Parket al. 2010; Feranie et al. 2011; Nakaya and Nakamura 2007). Therefore, by considering the same direction with alteration and fractures orientations, places that show more fractal dimension have more prone to mineralization by hydrothermal fluids & penetration.

Calculation of density, intensity and intersection for fractures was done in the Bajestan. Results revealed highest density (Fig. 4b), intensity (Fig. 4c) and intersection (Fig. 4d) values of fractures are the same as fractal analysis results (Fig. 4a). All of these results are evidences for further structural evolution, well-developed fractures and relating to alterations in the northwest and southeast of study area.

4. CONCLUSIONS

Through using the Spectral Angel Mapper classification (SAM) and RGB band combination, alteration zones consist of propylithic, phyllic, Argillic and Fe-oxides alterations were enhanced in the Bajestan. Results show the possibility of copper and iron mineralization in the area, particularly in the northwest and southeast of the study area. Applying spatial enhancement filters on the SPOT satellite data revealed the most fractures have NW-SE direction with a simple shear structural system.

Fractal dimension by using box counting method indicated that the most fractal dimension is 1.57 and the fractal dimension amounts increase in the west and southwest of the area. Statistical parameters such as fractures' intensity, fractures' density and fractures' intersection indicate a good match with fractal analysis results.

Integration of all data shows the most probability of mineralization was occurred along NW-SE direction. Field checking confirmed the results.

ACKNOWDEGMENT

The present study is based on the first author Ph.D. thesis at the Ferdowsi University of Mashhad, Mashhad, Iran with research number 18300.3; this study was supported by the Geological Survey of Iran (GSI). Meanwhile, GSI also provided the satellite data for this project.We are also thankful to University Technology Malaysia (UTM) and Korea Polar Research Institute (KOPRI) for their great assistance during preparation the manuscript.

REFERENCES

Abdi M and Karimpour M H., 2012. Application of Spectral Angel Mapper classification to discriminate hydrothermal alteration in SW Birjand, Iran by using ASTER image processing. Acta Geologica Sinica-English Edition 86(5):1289–1296. doi: 10.1111/j.1755-6724.2012.00748.x

Abrams A and Hook S., 2000. ASTER user handbook version2, jet propulsion laboratory 4800 oak grove Dr. Pasadena, CA 91109, bhaskar ramachandran, EROS data center Sioux falls, SD 57198:293-302.

Ashoori A R, Karimpour M H and Saadat S., 2008 Geological map of Bajestan scale: 1:100000. Geological survey of Iran.

Bedell R L., 2001. Geological mapping with ASTER satellite: new global satellite data that is a significant leap in remote sensing geologic and alteration mapping . Special Publication Geology Society of Nevada 33:329-334.

Berberian M, Jackson J A, Qorashi M, Khatib M M, Priestley K, Talebian M and Ghafuri-Ashtiani M., 1999. The 1997 may 10 Zirkuh (Qaenat) earthquake (Mw 7.2): faulting along the Sistan suture zone of eastern Iran. Geophysical Journal International 136:671-694.

Camp V and Griffis R., 1982. Character, genesis and tectonic setting of igneous rocks in the Sistan suture zone, eastern Iran. Lithous 15:221–239. doi:10.1016/0024-4937(82)90014-7
Di Tommaso I M and Rubinstein N., 2006. Hydrothermal alteration mapping using ASTER data in the Infiernillo porphyry deposit, Argentina. Journal of Ore Geology Reviews 29:1-16. doi:10.1016/j.oregeorev.2006.05.004
Eshghi Molan et al., 2014. Mineral mapping in the Maherabad area, eastern Iran, using the HyMap remote sensingdata. International Journal of Applied Earth Observation and Geoinformation 27:117-127. doi: 10.1016/j.jag.2013.09.014
Feranie S, Fauzi U and Bijaksana S.,2011. 3D fractal dimension and flow properties in the pore structure of geological rocks. Fractals 19:291-297. doi:10.1142/S0218348X1100535X
Hewson R D, CudahybT J, Mizuhiko S, Ueda K and Mauger A J., 2005. Seamless geologicalmap generation using ASTER in the Broken Hill–Curnamona province of Australia. Remote Sens. Environ. 99:159-172. doi:10.1016/j.rse.2005.04.025
Hirata T. (1989). Fractal dimension of fault systems in Japan: fractal structure in rock fracture geometry at various scales. Pure and Applied Geophysics 131:157–169 .
Iwasaki A and Tonooka H., 2005. Validation of a crosstalk correction algorithm for ASTER/SWIR. IEEE Transactions on Geoscience and Remote Sensing. 43(12): 2747-2751. doi:10.1109/TGRS.2005.855066
Jackson J, Haines J and Holt W. (1995). The accommodation of Arabia-Eurasia Plate convergence in Iran. Journal of Geophysical Research 100:205-215. doi: 10.1029/95JB01294
Karimpour m H, Malekzadeh-Shafaroudi A, Stern C R and Hidarian M R. (2008). Using ETM+ and airborne geophysics data to locating porphyry copper and epithermal gold deposits in Eastern Iran. Journal of Applied Science 8:4004–4016. doi:10.3923/ja
Liu R, Jiang Y, Li B and Xiaoshan W. (2015). A fractal model for characterizing fluid flow in fractured rock masses based on randomly distributed rock fracture networks. Computers and Geotechnics 65:45-55. doi:10.1016/j.compgeo.2014.11.004
Mars J C and Rowan L C. (2006). Regional mapping of phyllic- and argillic-altered rocks in the Zagros magmatic arc, Iran, using Advanced Spaceborne Thermal Emission and Reflection Radiometer (ASTER) data and logical operator algorithms. Geosphere 2:161-186. doi:10.1130/GES00044.1
Nakaya S and Nakamura K. (2007). Percolation conditions in fractured hard rocks: a numerical approach using the three-dimensional binary fractal fracture network (3D-BFFN) model,", B12203. Journal of Geophysical Research Solid Earth 112. doi:10.1029/2006JB004670
Ninomiya Y. (2002). Mapping quartz, carbonate minerals and mafic ultramafic rocks using remotely sensed multispectral thermal infrared ASTER data, Proceedings of SPIE. The International Society for Optical Engineering 4710:191-202. doi:10.1117/12.459566
Ninomiya Y. (2003). A stabilized vegetation index and several mineralogic indices defined for ASTER VNIR and SWIR data. " Proc. IEEE 2003 International Geoscience and Remote Sensing Symposium (IGARSS'03) 3:1552-1554.
Ninomiya Y. (2004). Lithologic mapping with multispectral ASTER TIR and SWIR data," Proceedings of SPIE. The International Society for Optical Engineering 5234:180–190. doi:10.1117/12.511902
Pour A B and Hashim M. (2012). The application of ASTER remote sensing data to porphyry copper and epithermal gold deposits. Ore Geology Review 44:1-9. doi:10.1016/j.oregeorev.2011.09.009
Pour B A, Hashim M and Marghany M. (2011). Using spectral mapping techniques on short wave infrared bands of ASTER remote sensing data for alteration mineral mapping in SE Iran . Int. J. Phys. Sci. 6 (4):917–929. doi:10.5897/IJPS10.510
Pourlatifi A . (2002). Geological map of Ferdows. Geological survey of Iran, scale: 1:100000.
Ram A, and Roy P N S. (2005). Fractal dimensions of blocks using a box-counting technique for the 2001 Bhuj earthquake, Gujarat. Pure and applied geophysics 162:531-548. doi:10.1007/s00024-004-2620-4
Rockwell B W and Hofstra A H. (2008). Identification of quartz and carbonate minerals across northern Nevada using ASTER thermal infrared emissivity data implications for geologic mapping and mineral resource investigations in well-studied and frontier areas. Geosphere 4(1):218-246. doi:10.1130/GES00126.1
Rowan L C and Mars J. (2003). CLithologic mapping in the Mountain Pass, California area using Advanced Spaceborne Thermal Emission and Reflection Radiometer (ASTER) data. Remote Sensing Environ. 84:350-366. doi:10.1016/S0034/-4257(02)00127-X
Rowan L C, Schmidt R G and Mars J C. (2006). Distribution of hydrothermally altered rocks in the Reko Diq, Pakistan mineralized area based on spectral analysis of ASTER data. Remote Sensing of Environment 104(1):74-87. doi:10.1016/j.rse.2006.05.014
Rowan L,Hook S J, Abrams M J, and Mars J C. (2003). Mapping hydrothermally altered rocks at Cuprite, Nevada, using the Advanced Spaceborne thermal emission and reflection radiometer (ASTER), a new satellite-imaging system . Econ. Geol. Bull. Soc. Econ 98(5):1019-1027. doi:10.2113/98.5.1019
Sabins F F. (1999). Remote sensingfor mineral exploration. Ore Geology Reviews 14:157–183. doi: 10.1016/S0169-1368(99)00007-4

Tangestani M H, Mazhari N, Ager B and Moore F. (2008). Evaluating advance spaceborne thermal emission and reflection radiometer (ASTER) data for alteration zone enhancement in a semi-arid area, northern Shahr-e-Babak, SE Iran. Int. J. Remote. Sens. 29(10):2833-2850. doi:10.1080/01431160701422239
Tirrul R, Bell I R, Griffis R J, and Camp V E. (1983). The Sistan suture zone of Eastern Iran. Geological Society of America Bulletin 94:134–156. doi:10.1130/0016-7606(1983)94<134:TSSZOE>2.0.CO;2
Velosky J C, Stern R J and Johnson P R. (2003). Geological control of massive sulfide mineralization, in the Neoproterozoic Wadi Bidah shear zone, southwestern Saudi Arabia,inferences from orbital remote sensing and field studies. Precambrian Res. 123(2-4):235-247. doi:10/1016/S0301-9268(03)00070-6
Vincent R K. (1997). Fundamentals of Geological and Environmental Remote Sensing, Prentice Hall, Upper Saddle River, New Jersey. doi:10.1017/S0016756898391505
Yamaguchi Y and Naito C. (2003). Spectral indices for lithologic discrimination and mapping by using the ASTER SWIR bands. Int. J. Remote. Sens. 24 (22):4311–4323. doi:10.1080/01431160110070320
Zhang X and Sanderson D J. (1998). Numerical study of critical behaviour of deformation and permeability of fractured rock masses. Marine and Petroleum Geology 15:535–548. doi:10.1016/S0264-8172(98)00030-0